Development 140, 4060-4069 (2013) doi:10.1242/dev.096651

The F-box protein ZEITLUPE controls stability and nucleocytoplasmic partitioning of GIGANTEA

Jeongsik Kim[1], Ruishuang Geng[1], Richard A. Gallenstein[1] and David E. Somers[1,2,*]

SUMMARY

Nucleocytoplasmic partitioning of core clock components is essential for the proper operation of the circadian system. Previous work has shown that the F-box protein ZEITLUPE (ZTL) and clock element GIGANTEA (GI) heterodimerize in the cytosol, thereby stabilizing ZTL. Here, we report that ZTL post-translationally and reciprocally regulates protein levels and nucleocytoplasmic distribution of GI in *Arabidopsis*. We use ectopic expression of the N-terminus of ZTL, which contains the novel, light-absorbing region of ZTL (the LOV domain), transient expression assays and *ztl* mutants to establish that the levels of ZTL, a cytosolic protein, help govern the abundance and distribution of GI in the cytosol and nucleus. Ectopic expression of the ZTL N-terminus lengthens period, delays flowering time and alters hypocotyl length. We demonstrate that these phenotypes can be explained by the competitive interference of the LOV domain with endogenous GI-ZTL interactions. A complex of the ZTL N-terminus polypeptide with endogenous GI (LOV-GI) blocks normal GI function, causing degradation of endogenous ZTL and inhibition of other GI-related phenotypes. Increased cytosolic retention of GI by the LOV-GI complex additionally inhibits nuclear roles of GI, thereby lengthening flowering time. Hence, we conclude that under endogenous conditions, GI stabilization and cytoplasmic retention occurs naturally through a LOV domain-mediated GI-ZTL interaction, and that ZTL indirectly regulates GI nuclear pools by sequestering GI to the cytosol. As the absence of either GI or ZTL compromises clock function and diminishes the protein abundance of the other, our results highlight how their reciprocal co-stabilization is essential for robust circadian oscillations.

KEY WORDS: Circadian biology, F-box protein, GIGANTEA, Nucleocytoplasmic partitioning, *Arabidopsis, Nicotiana benthamiana*

INTRODUCTION

The regulation of protein turnover and nucleocytoplasmic distribution is part of the molecular mechanism at the core of the circadian clock (Harmer, 2009; Herrero and Davis, 2012; Más, 2008; Tataroğlu and Schafmeier, 2010). F-box proteins are key components of SCF-type E3 ligases that target proteins for degradation via the 26S proteasome pathway and play a substantial role in all circadian systems (Godinho et al., 2007; He et al., 2003; Ko et al., 2002; Koh et al., 2006; Siepka et al., 2007; Somers et al., 2000). The cytosol-localized F-box protein ZEITLUPE (ZTL) is the defining component of the SCF^{ZTL} E3 ligase, which regulates degradation of TIMING OF CAB2 EXPRESSION (TOC1) and PSEUDO RESPONSE REGULATOR5 (PRR5), two evening-phased circadian clock components (Fujiwara et al., 2008; Kiba et al., 2007; Kim et al., 2007; Más et al., 2003). Additionally, PRR5 enhances TOC1 protein by facilitating nuclear import of TOC1, sequestering both proteins from proteolysis by SCF^{ZTL} (Wang et al., 2010). Hence, the cytosolic localization of ZTL highlights the importance of protein compartmentalization in the regulation of clock activity.

ZTL belongs to a small, unique family of F-box proteins [ZTL, FLAVIN BINDING, KELCH REPEAT, F-BOX1 (FKF1) and LOV KELCH PROTEIN2 (LKP2)] containing a LOV (light, oxygen or voltage sensing) domain at the N-terminus, followed by an F-box domain and six kelch repeats (Demarsy and Fankhauser, 2009; Ito et al., 2012). The ZTL LOV domain shares high homology with the LOV domains of plant phototropins and WHITE COLLAR-1 (WC-1) in *Neurospora* (Ballario et al., 1996; Crosson et al., 2003; Ito et al., 2012). The LOV domains in these proteins bind to flavins and function as a light-driven molecular switch in light-mediated protein activation (He et al., 2002; Imaizumi et al., 2003; Matsuoka and Tokutomi, 2005).

LOV domains also mediate protein-protein interactions, including homodimerization of WC-1 and the phototropins (Ballario et al., 1998; Nakasako et al., 2008). ZTL binding to GIGANTEA (GI) in blue light requires a functional LOV domain, and LOV mutations that abolish flavin binding diminish the interaction and eliminate blue light-enhanced interactions (Kim et al., 2007). The ZTL-GI interaction stabilizes ZTL protein in the light and ensures robust oscillation of its target proteins (Kim et al., 2007). Similar LOV domain-mediated interactions take place between FKF1 and GI to influence *CONSTANS* (*CO*) expression and protein abundance in the regulation of photoperiodic flowering (Imaizumi et al., 2005; Sawa et al., 2007; Song et al., 2012). In long days, an FKF1-GI complex forms in the nucleus, degrading transcriptional repressors of *CO* and activating *CO* expression, which, in turn, promotes *FT* expression and flowering (Imaizumi et al., 2005; Sawa et al., 2007).

In this study, we identify a new post-transcriptional step in GI regulation. We show that ectopic expression of the ZTL N-terminus (LOV domain) competitively interferes with endogenous GI-ZTL interactions, simultaneously promoting ZTL degradation and inhibiting GI functions. Furthermore, under endogenous expression levels, GI stabilization and cytoplasmic retention occurs through a LOV domain-mediated GI-ZTL interaction. These reciprocal co-enhancements in the cytosol help maintain a strong oscillation of the GI-ZTL complex, contributing to the robustness of the circadian system.

[1]Department of Molecular Genetics, Ohio State University, Columbus, OH 43210, USA. [2]Integrative Biosciences and Biotechnology, Pohang University of Science and Technology, Hyojadong, Pohang, Kyungbuk, 790-784, Republic of Korea.

*Author for correspondence (somers.24@osu.edu)

Accepted 22 July 2013

MATERIALS AND METHODS

Plasmid construction and plant materials

The *35S:LOV* and *35S:LOV-F* constructs to generate *Arabidopsis* transgenic line expressing the LOV (1-192 aa) and LOV-F-box (1-280 aa) polypeptides under the control of the *35S* promoter were generated as described previously (Han et al., 2004). In short, a C-terminal c-myc-tagged *35S:LOV* construct was created by digesting the full length ZTL cDNA in pRTL2 with *Bso*BI and *Xba*I to remove the C-terminal region and fusing the first 192 residues to a single c-myc tag (LOV). Similarly, *Xba*I and *Xmn*I were used to fuse the N-terminal 280 residues (LOV-F) to a c-myc tag. These constructs were subcloned into pZP200 and transformed into *Arabidopsis* (Columbia) containing *CAB2:LUC* using standard techniques (Clough and Bent, 1998).

The constructs of full-length genes, deletions of *ZTL* and *FKF1* and their mutants for transient expression in *Nicotiana benthamiana* or in *Arabidopsis* mesophyll protoplasts were prepared using the gateway system (Invitrogen). Entry clones for *ZTL*, *ZTL-KELCH*, *ZTL-LOV*, *ZTL(G46E)-LOV*, *FKF1-LOV* and *FKF1* were generated by PCR with *Pyrococcus furiosus* (Pfu) DNA polymerase (Stratagene), using plasmids containing full-length protein-coding sequences of *ZTL*, *FKF1* and *ZTL(G46E)* (Kim et al., 2007) as templates and cloned into pCR-CCD-F. The primer pairs used for plasmid construction are listed (supplementary material Table S1). The final constructs were established by the LR recombinase reaction using each entry clone and the Gateway version of pCsVMV:GFP-C-999 or pCsVMV:HA-C-1300 as destination vectors for *Arabidopsis* protoplast expression and for tobacco infiltration, respectively. *35S:GI-GFP* has been described (Kim et al., 2007).

phyB-101 (Col) and *cry1-304* (Col) were obtained from the *Arabidopsis* Biological Resource Center and Dr C. Lin (UCLA, USA), respectively. *ztl-103*, *GI:GI-HA* and *35S:GI-GFP* have been described previously (David et al., 2006; Kim et al., 2007). *GI:GI-HA LOV-OX* and *35S:GI-GFP ztl-103* were generated by genetic crossing between *GI:GI-HA* and *LOV-OX* (87-16) and between *35S:GI-GFP* and *ztl-103*, respectively. All lines were confirmed by either PCR-based genotyping or their resistance to antibiotics.

Protein extraction, fractionation, immunoblot and immunoprecipitation analyses

Protein extraction, immunoblot and immunoprecipitation analyses were performed as described previously with minor modifications (Kim et al., 2007). For co-immunoprecipitation of GI and LOV, formaldehyde treatment was performed for tissue-crosslinking. *Arabidopsis* seedlings were grown for 10 days in a 12-hour light/12-hour dark photoperiod and then harvested at zeitgeber time (ZT)13. The seedlings were soaked in 20 ml of ice-cold 1× PBS (140 mM NaCl, 2.7 mM KCl, 10 mM Na_2HPO_4 and 1.8 mM KH_2PO_4) containing 1% formaldehyde and vacuum-infiltrated for 30 minutes in an ice bath. Ice-cold glycine was added to bring the final concentration to 300 mM and then the vacuum infiltration was continued for 30 minutes. Following the infiltration, the seedlings were washed three times in 1× PBS and then frozen in liquid nitrogen for further protein analysis. For immunoprecipitation, protein extracts were prepared using extraction buffer (50 mM Tris-HCl, pH 7.5, 150 mM NaCl, 0.5% Nonidet P-40, 1 mM EDTA, 1 mM dithiothreitol, 1 mM phenylmethylsulfonyl fluoride, 5 μg/ml leupeptin, 1 μg/ml aprotinin, 1 μg/ml pepstatin, 5 μg/ml antipain, 5 μg/ml chymostatin, 50 μM MG132, 50 μM MG115 and 50 μM ALLN) and immunoprecipitations were performed with anti-HA as described previously. Immunodetection using anti-HSP90 (1:50,000), anti-ADK (1:40,000), anti-Histone 3 (1:40,000), anti-ZTL (1:500) and anti-HA (1:1000) was performed as described previously except for different dilutions.

Isolation of nuclear and cytosolic proteins for tobacco tissue and nuclear proteins for *Arabidopsis* was performed with a CelLytic PN Isolation/Extraction Kit (Sigma-Aldrich) as previously described (Wang et al., 2010) with minor modifications. Isolation of cytosolic protein from *Arabidopsis* was carried out as previously described (Kim et al., 2007) but using 1× nuclei isolation buffer of the CelLytic PN Isolation Extraction Kit (Sigma-Aldrich). Purification of each compartment was validated by immunodetection using cytosolic (ADK) and nuclear (Histone H3) marker proteins.

Hypocotyl elongation, period analysis and flowering time measurement

For the hypocotyl elongation assay, seeds plated on medium with 1× MS salts, 3% sucrose and 0.8% agar were incubated at 4°C for 3 days and germinated under white light at 23°C for 8 hours before being transferred into a growth chamber with constant blue or red light. Different light intensities were achieved by covering the plates with neutral density filters [Roscolux 397 (Rosco Laboratories, Stamford, CT)]. Hypocotyl length was measured after 7 days incubation using a ruler.

The free-running period of transgenic plants was determined using *CAB2:luciferase* (*CAB2:LUC*) as a bioluminescent reporter as previously described (Somers et al., 2004).

For flowering time measurement, seeds were sterilized and plated on MS medium (0.8% agar) supplemented with 3% sucrose and cold-treated for 4 days before being moved to long days (16-hour light/8-hour dark, 70-100 μmol m^{-2}) or short days (8-hour light/16-hour dark, 100 μmol m^{-2}). After 7 days of growth, seedlings were transplanted to soil and were grown in the same light condition until flowering. Total numbers of rosette and cauline leaves were counted when the bolts were about 1 cm in length.

Analysis of mRNA level

Analysis of transcript level was performed using RNA gel blot analysis for *ZTL*, semi-quantitative RT-PCR for *CO* and *FT* as previously described (Somers et al., 2004) and quantitative real-time PCR for *GI-HA* as previously described (Kim et al., 2008). *Arabidopsis* seedlings were grown for 10 days in a 12-hour light/12-hour dark photocycle and then harvested as indicated. Total RNA was extracted using Trizol Reagent (Invitrogen) or TRI reagent (MRC) according to the manufacturer's instructions, and further treated with DNase (Ambion) before RT-PCR and q-PCR analysis. An equal amount (~400 ng) of total RNA was used for generating cDNA using the SuperScript III Kit (Invitrogen). Real-time PCR was performed using IQ SYBR Green Supermix (Biorad) and an iQ5 real-time PCR detection system (Bio-Rad). The reaction protocol for the q-PCR reaction proceeded as follows: 94°C for 2 minutes, followed by 40 cycles of 94°C for 15 seconds and 60°C for 34 seconds. The relative expression of target genes between samples was normalized to *ACT2* expression, and further normalized to the maximum level among their relative expression for each trial. The primer pairs used in the PCR analyses are listed (supplementary material Table S1).

Transient expression in protoplasts and *N. benthamiana* and microscopy

Protoplast preparation and DNA transfection was performed as previously described with a minor modification (Kim et al., 2008; Kim and Somers, 2010). *GI:GI-HA* plants were grown for 20-30 days in a 12-hour light/12-hour dark photoperiod. Preparation of *Arabidopsis* protoplasts started at ZT7 and DNA transfection ended at ZT11-12. About 400 μl protoplast solution with 10^5 protoplast cells and ~90-140 μg DNA for effectors depending on plasmid size were used per reaction. After a 24-hour incubation in the same chamber where plants were grown, protoplasts were harvested.

For microscopy imaging, transient expression in *N. benthamiana* was performed using p19-enhanced Agrobacteria infiltration (Voinnet et al., 2003). Agrobacteria containing the plasmids *35S:GI-GFP* alone (plus *35S:H2B-RFP* and *35S:P19*) or *35S:GI-GFP* and *CsVMV:HA-ZTL-LOV* (plus *35S:H2B-RFP* and *35S:P19*) were co-infiltrated into *N. benthamiana* plants. Images were captured 2 days after infiltration using an E600 fluorescence microscope (Nikon, Japan) with proper filter sets and Advanced SPOT Software (Diagnostics Instruments). The intensity of fluorescent signals was plotted using ImageJ software.

RESULTS

Circadian clock-related phenotypes in ZTL-LOV-OX plants

The ZTL LOV domain is essential for stabilizing ZTL levels through interaction with GIGANTEA (GI) (Kim et al., 2007). To investigate further the functional role of the ZTL LOV domain, we

generated transgenic plants ectopically expressing the LOV (ZTL-LOV; 1-192 aa) and LOV-F (ZTL-LOV-F; 1-280 aa) domains. Because the F-box portion of all F-box proteins interacts with the SKP1 protein within the context of the SCF ubiquitin ligase complex, we tested whether this domain might affect the phenotype, possibly by sequestering LOV-F into SCF complexes. This could have a great effect on SCF ubiquitin ligase function in the plant, by 'poisoning' SCF complexes in all contexts of its ligase function. We characterized four transgenic lines expressing the 20-kDa LOV domain (LOV-OX) and three lines expressing the 26-kDa LOV-F (LOV-F-OX) domain (supplementary material Fig. S1) for effects on circadian cycling, flowering time and photomorphogenesis.

Disruption of clock function often alters circadian period and/or amplitude, accompanied by changes in hypocotyl elongation and flowering time (Yakir et al., 2007). ZTL loss-of-function mutations lengthen the free-running period by several hours, whereas constitutive expression of full-length ZTL shortens this period or causes arrhythmicity (Somers et al., 2004). We tested several LOV and LOV-F transgenic lines for period alteration under constant red or blue light after entrainment in 12-hour light/12-hour dark cycles. Under constant red light, the LOV-OX and LOV-F-OX lines have a free-running period ~0.5-2 hours longer than that of wild type (WT) (Fig. 1A). Under constant blue light, the period was also lengthened by 1-2.5 hours (Fig. 1B).

We next examined flowering time in these lines when grown under long (16-hour light/8-hour dark) or short (8-hour light/16-hour dark) days. Similar to ZTL overexpressors (ZTL-OXs), both LOV-OX and LOV-F-OX lines flowered late in long days compared with WT, with little effect in short days (Fig. 1C). Photoperiodic control of flowering time is mainly regulated by *CONSTANS* (*CO*) and *FLOWERING LOCUS T* (*FT*) (Mouradov et al., 2002). In both transgenic types, *CO* and *FT* expression was strongly reduced during long photoperiods (Fig. 1D,E). These reductions are similar to that found in ZTL-OXs (Somers et al., 2004), or other late-flowering mutants with altered clock activity (Mouradov et al., 2002).

Overexpression of ZTL lengthens hypocotyls in either red or blue light (Somers et al., 2004). We tested the effect of LOV and LOV-F overexpression on hypocotyl growth under these conditions. In red light, both types of plants have slightly longer hypocotyls at all but the very highest fluence rates (Fig. 1F,G). These effects are phytochrome B (phyB)-dependent, as *phyB* is epistatic to both OX types (Fig. 1F,G). Similar lengthening effects were obtained under blue light (Fig. 1H,I) except that the *cryptochrome1* (*cry1*) mutation additively lengthens the effect of LOV/LOV-F backgrounds. This indicates that blue light signaling via a LOV/LOV-F pathway is parallel to CRY1 signaling, consistent with LOV/LOV-F disruption of phytochrome signaling (Neff and Chory, 1998).

Taken together, the three phenotypes examined in the LOV-OX and LOV-F-OX lines cannot be explained by simple dominant-negative or gain-of-function effects of LOV-OX on ZTL. The lengthened period of LOV- and LOV-F-OXs is similar to that of *ztl* loss-of-function mutants, but the late flowering and hypocotyl lengthening phenocopies ZTL overexpression (Somers et al., 2004). Instead, these results might arise from a combination of effects of the LOV and LOV-F domains on ZTL and/or an interacting protein, such as GI.

Competitive interaction of LOV proteins with GI reduces ZTL levels

We measured the level of endogenous ZTL protein in the LOV-OXs and LOV-F-OXs to determine whether the longer period resulted from lower endogenous ZTL. In all lines tested, ZTL levels were

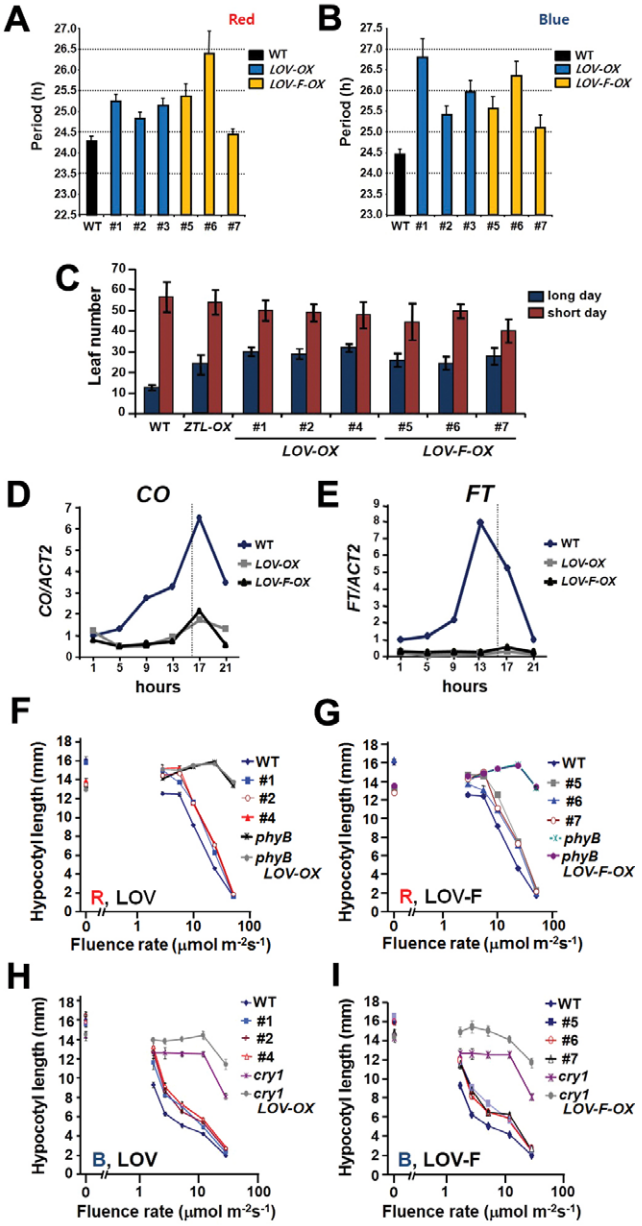

Fig. 1. Expression of LOV and LOV-F domains of ZTL alters circadian clock-related phenotypes in *Arabidopsis*. (**A**,**B**) Period length of transgenic lines expressing ZTL LOV or LOV-F polypeptides in constant red (A) and blue (B) light. *LOV-OX* and *LOV-F-OX* were entrained in a 12-hour light/12-hour dark (LD) photoperiod for 7 days, and released in constant light as indicated. Three *LOV-OX* lines (#1, #2, #3; blue bars) and three *LOV-F-OX* lines (#5, #6, #7; yellow bars) are shown. Data are variance-weighted means (±s.e.m.) of three trials. (**C**) Flowering time of *LOV-OX* and *LOV-F-OX* in long and short days. Total number of leaves (rosette and cauline) of WT, ZTL overexpressor (*ZTL-OX*), *LOV-OX* and *LOV-F-OX* were counted at flowering under long (dark blue) and short (dark red) days. Values (means ± s.e.m.; *n*=12-18) are representative of two experiments. (**D**,**E**) Expression levels of *CO* (D) and *FT* (E) transcripts from WT, *LOV-OX* (#1) and *LOV-F-OX* (#5) seedlings grown for 8 days in long days. Relative expression of *CO* and *FT* was normalized to *ACTIN2*. Data are representative of two independent trials. (**F-I**) Hypocotyl elongation of WT, *LOV-OX*, *LOV-F-OX*, *phyB*, *phyB*LOV and *phyB*LOV-F in red light (F,G) and the same OX lines with *cry1*, *cry1*LOV and *cry1*LOV-F in blue light (H,I). Seedlings were grown for 10 days under constant red (F,G) or blue (H,I) light. Unconnected data points show hypocotyl length of dark-grown seedlings. Values (means ± s.e.m.) are representative of two trials; *n*=16-29.

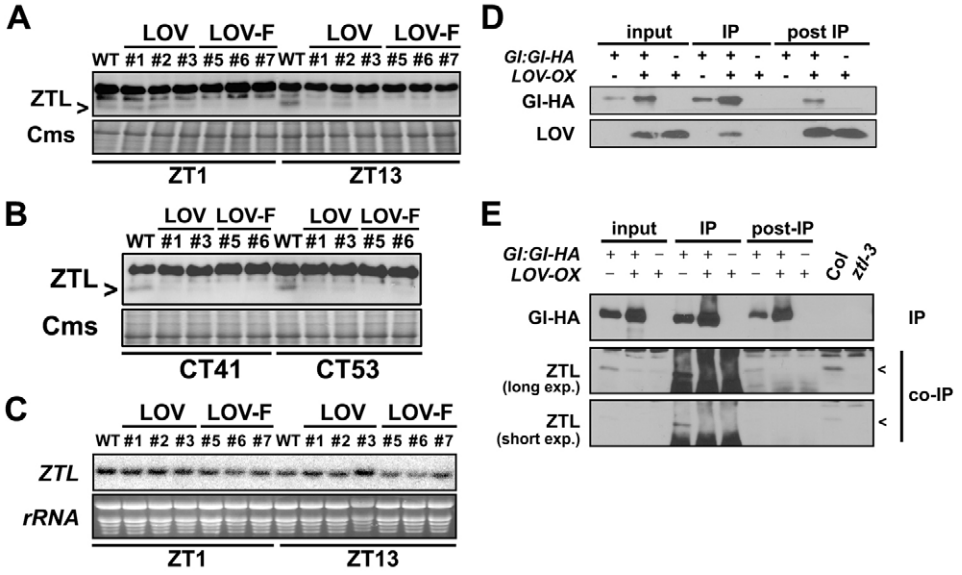

Fig. 2. Post-transcriptional reduction of endogenous ZTL in LOV-OX and LOV-F-OX *Arabidopsis* plants through competitive interaction with GI. (**A**,**B**) Abundance of ZTL in *LOV-OX* and *LOV-F-OX*. Endogenous ZTL levels from indicated genotypes grown under LD and harvested at ZT1 and ZT13 (A) and at CT41 and CT53 (B) in constant blue light as determined by immunoblotting. Cms, Coomassie-stained bands; ZT, zeitgeber time; CT, circadian time. (**C**) *ZTL* transcript levels in *LOV-OX* and *LOV-F-OX*. *ZTL* mRNA levels in seedlings grown as in A were analyzed by RNA gel blot. Lower panel shows rRNA as loading control. (**D**,**E**) Co-IP analysis of GI-HA and either LOV (D) or endogenous ZTL (E). Protein expression from cross-linked (D) or non-cross-linked (E) tissues of *GI:GI-HA*, *GI:GI-HAxLOV-OX* and *LOV-OX* plants grown in LD and harvested at ZT13 was determined by immunoblotting. Soluble fraction (input), eluates (IP) and supernatant fraction after IP (post-IP) are shown. Arrowheads show ZTL position.

strongly reduced or undetectable compared with WT plants grown under a 12-hour light/12-hour dark (LD) photoperiod (Fig. 2A) or under constant blue light (Fig. 2B). In LD cycles, the relative decrease was stronger at ZT13, compared with ZT1, especially in LOV-OX lines (Fig. 2A). However, in constant light, ZTL levels were similarly very low in all lines (Fig. 2B). *ZTL* mRNA in these transgenic lines showed no consistent differences from WT (Fig. 2C), indicating a post-transcriptional mechanism.

Because ZTL is stabilized in blue light by binding to GI via the LOV domain (Kim et al., 2007), we next tested whether lower ZTL resulted from the competitive binding of LOV and LOV-F proteins to GI. Co-immunoprecipitations (co-IPs) were performed using plants expressing both ZTL-LOV and GI-HA, ZTL-LOV alone, or GI-HA alone. ZTL-LOV polypeptides co-immunoprecipitated with GI-HA only in plants expressing both ZTL-LOV and GI-HA (Fig. 2D), confirming that the LOV domain of ZTL alone is sufficient to bind GI *in vivo* (Kim et al., 2007). Additionally, the amount of endogenous ZTL co-immunoprecipitated with GI was significantly reduced in the *GI:GI-HAxLOV-OX* line compared with the *GI:GI-HA* line (Fig. 2E), even though precipitated GI is much higher in *GI:GI-HAxLOV-OX*. This suggests that a strong ZTL-LOV interaction with GI competes with ZTL for GI binding, reducing access of endogenous ZTL to GI and resulting in ZTL degradation and a longer circadian period.

Stabilization of GI by ZTL through a LOV-mediated interaction

GI protein, but not *GI* message, is reduced in *ztl* mutants, suggesting that GI levels might be regulated by ZTL post-transcriptionally (Kim et al., 2007). We performed immunoblot analyses to determine the effect of LOV overexpression on GI protein accumulation. GI-HA levels are significantly increased in lines expressing LOV polypeptide relative to the untransformed *GI:GI-HA* line over the entire LD time course (Fig. 3A). *GI-HA* mRNA remains unchanged in the LOV-OX background (Fig. 3B; supplementary material Fig. S2), indicating that ZTL-LOV stabilizes GI post-transcriptionally.

We then tested whether a direct interaction between ZTL-LOV and GI is necessary to stabilize GI protein and whether ZTL has a specific role in this process. We analyzed GI-HA protein levels at ZT12 in *GI:GI-HA* protoplasts transiently transfected with ZTL- and FKF1-related constructs as effectors including GFP, GFP-ZTL-LOV, GFP-ZTL(G46E)-LOV, GFP-FKF1-LOV, GFP-ZTL and GFP-ZTL(G46E). FKF1 also binds GI through its LOV domain, but is nuclear-localized and controls flowering time without affecting circadian period (Sawa et al., 2007). A predicted, nuclear localization signal exists at the N-terminus of FKF1 (supplementary material Fig. S3A); this was confirmed by observing nucleus-enriched fluorescent signals when GFP-tagged FKF1-LOV (GFP-FKF1-LOV) or FKF1 (GFP-FKF1) were transiently expressed in *N. benthamiana*. These localization patterns are very different from the cytosol-enriched fluorescent signals seen with GFP-ZTL-LOV and GFP-ZTL (supplementary material Fig. S3B). We also tested the effect of the G46E mutation, which disrupts the ZTL-GI interaction (Kim et al., 2007).

The abundance of GI-HA protein varied depending on the effector, although all effector proteins were expressed well, with higher levels of LOV polypeptides and lower levels of full-length proteins (Fig. 3C). Compared with the GFP-transfected controls, GI-HA levels were markedly increased in *GI:GI-HA* protoplasts transfected with GFP-ZTL-LOV and GFP-ZTL, with fourfold and twofold enrichments, respectively (Fig. 3D,E). By contrast, the non-interacting GFP-ZTL(G46E) and GFP-ZTL(G46E)-LOV mutants showed little or no GI enhancement relative to the effects of the GFP control (Fig. 3D,E). In addition, FKF1-LOV had little effect on GI stabilization, similar to that of ZTL(G46E)-LOV and much less than that of ZTL-LOV, although all three polypeptides were

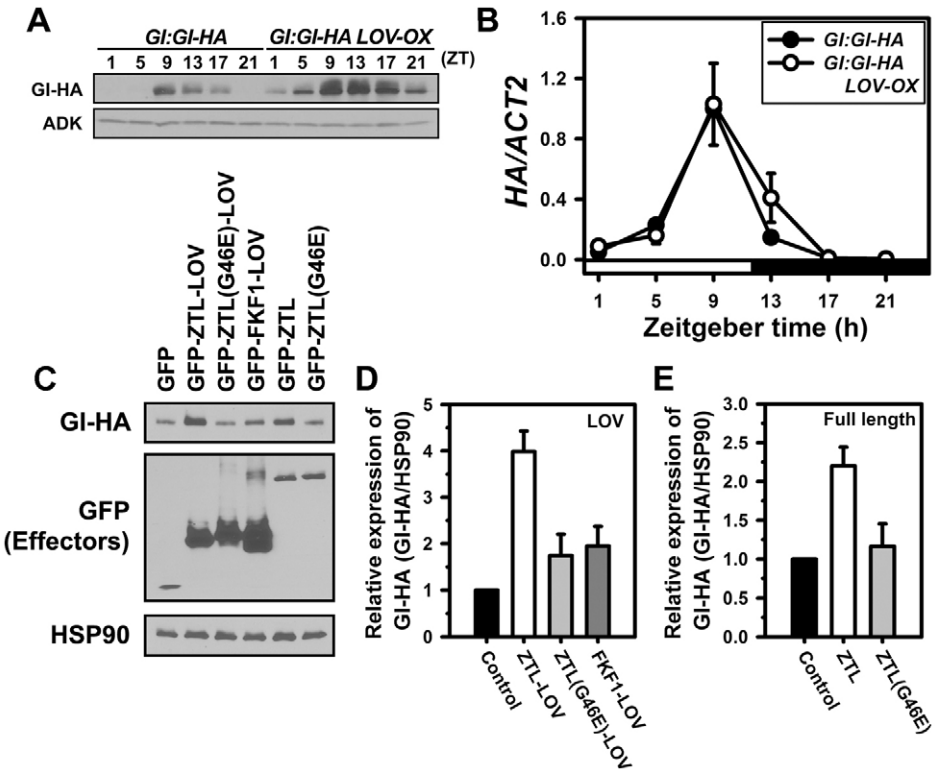

Fig. 3. LOV domain-mediated ZTL binding to GI accumulates GI protein. (**A**,**B**) Expression level of *GI-HA* protein (A) and mRNA (B) in *GI:GI-HA* and *GI:GI-HAxLOV-OX Arabidopsis* plants. Seedlings were grown for 10 days in LD and harvested as indicated times (ZT). (A) GI-HA levels were determined from total protein extracts by immunoblotting. ADK was used as loading control. Data are representative of two trials. (B) *GI-HA* mRNA levels were determined by quantitative real-time PCR using specific primers for HA tag. Relative expression of *GI-HA* was normalized to *ACT2* and then scaled to the highest level among WT samples (ZT9) within a trial. White and black bars indicate light and dark, respectively. Data are means ± s.e.m. (n=2). (**C-E**) GI-HA in *GI:GI-HA* protoplasts transfected with *LOV* (C,D) and full-length (C,E) *ZTL* or *FKF1* and their mutants. Mesophyll protoplasts were extracted from *GI:GI-HA* leaves entrained in LD and transfected with *GFP*, *GFP-ZTL-LOV*, *GFP-ZTL(G46E)-LOV*, *GFP-FKF1-LOV*, *GFP-ZTL* and *GFP-ZTL(G46E)* under the control of *CsVMV* promoter as effectors. GI-HA and GFP-ZTL and GFP-FKF1 were detected by immunoblotting of total protein extracts from protoplasts of the respective transfection. Loadings are normalized to HSP90. Images are representative of four trials. D and E show quantification of relative GI expression from C. GI levels in each sample were normalized to HSP90 and further normalized to GFP-transfected control within a trial. Data are means ± s.e.m. of four independent trials.

similarly strongly expressed (Fig. 3C,D). These results, together with our previous report of GI-mediated ZTL stabilization, suggest that ZTL and GI co-stabilize through LOV domain-mediated direct interaction.

A ZTL-GI interaction enhances GI cytosolic localization

GI is stabilized more effectively by cytosolic ZTL-LOV than by nuclear FKF1-LOV, so we hypothesized that ZTL regulates both the stability of cytosolic GI and its nucleocytoplasmic distribution. We measured the ratio of cytosolic to nuclear GI by fractionating cytosolic and nuclear proteins from *N. benthamiana* leaves transiently expressing GI-GFP in the presence of ZTL- or FKF1-related derivatives as effectors (Fig. 4A,B). Co-expression of GI-GFP with HA-ZTL-LOV increases cytosolic GI levels relative to nuclear protein levels, whereas expression of GI-GFP with HA-ZTL-KELCH, HA-ZTL(G46E)-LOV or HA-FKF1-LOV have little or no effect on nuclear and cytosolic GI levels (Fig. 4A,C). Similar changes in GI nucleocytoplasmic partitioning were observed when full-length HA-ZTL was expressed, but not when HA-ZTL(G46E) or HA-FKF1 were expressed as effectors (Fig. 4B,C). Both full-length ZTL and the ZTL-LOV domain increase the relative cytosolic distribution of GI-GFP significantly, with the effect of the ZTL-LOV domain being markedly stronger than full length ZTL. By contrast, full-length FKF1 and the LOV domain of FKF1 have a slight effect on GI localization. However, neither the ZTL C-terminus (KELCH) nor ZTL mutant (G46E) altered GI nucleocytoplasmic partitioning. These results tie the effectiveness of cytosolic retention of GI to its ability to interact with ZTL. We confirmed these fractionation experiments *in planta* by observing more GI-GFP fluorescence in the cytosol and less fluorescence in the nucleus when ZTL-LOV was expressed as an effector (Fig. 4D). We also found that light quality had no effect on ZTL-LOV-dependent partitioning of GI (supplementary material Fig. S4).

An enhanced ratio of cytosolic to nuclear GI by ZTL-LOV or full-length ZTL protein could result from the protection of cytosolic GI from degradation and/or from the sequestration of GI to the cytosol. We next tested the effect of different ZTL-LOV levels on the accumulation of GI-GFP protein in the nucleus and cytosol. As the relative amount of ZTL-LOV was increased, there was a corresponding increase of cytosolic GI and a concomitant reduction in nuclear GI protein (Fig. 4E, compare levels 0 with 4). These different compartmental responses of GI are likely to be due to ZTL effects on both GI cytosolic retention and protein stabilization.

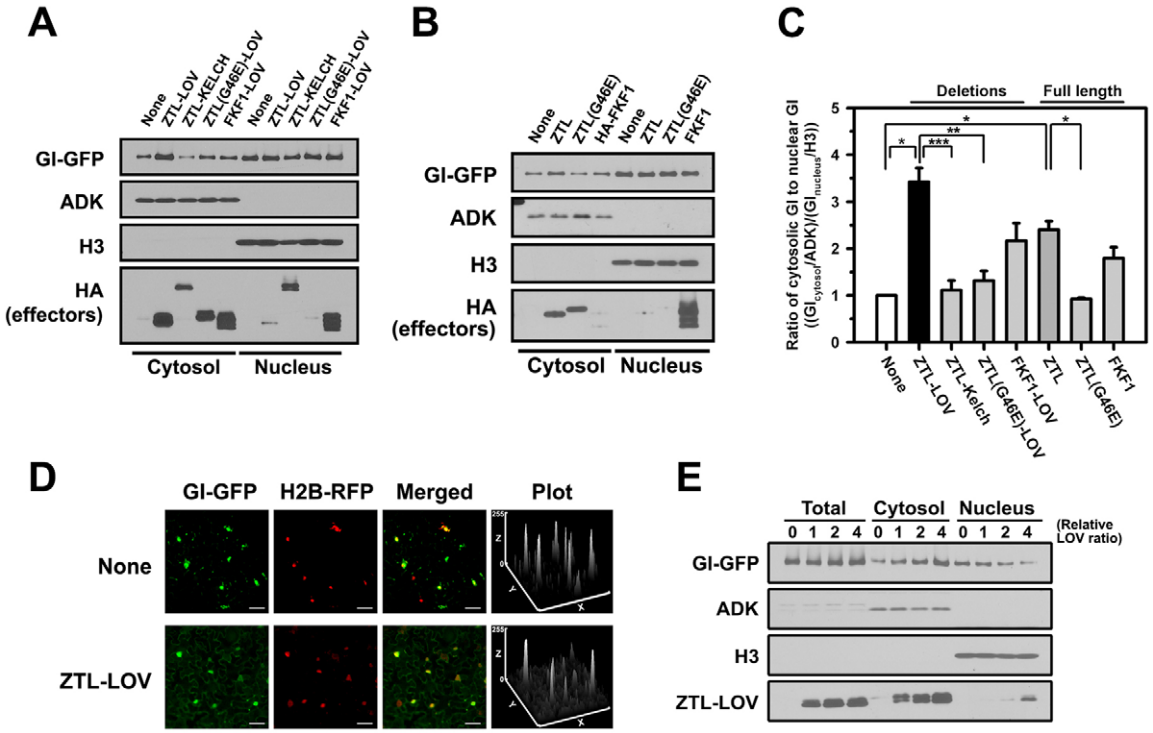

Fig. 4. ZTL alters the GI nucleocytoplasmic distribution through a LOV-mediated interaction. (**A-C**) Cytosolic and nuclear GI-GFP protein levels in *N. benthamiana* transiently expressing GI-GFP along with truncated (A) and full-length (B) HA-ZTL or HA-FKF1 and select mutants as effectors. *35S:GI-GFP* was co-expressed with deleted and full-length forms of *CsVMV:HA-ZTL* or *CsVMV:HA-FKF1* plasmids in *N. benthamiana* and protein levels determined by immunoblotting. Data are representative of three trials. (C) Quantification of ratios of cytosolic to nuclear GI level from A,B. Levels of cytosolic and nuclear GI protein were normalized to ADK and H3, respectively, and further normalized to empty vector (None) within a trial. Bars show means ± s.e.m. of three independent trials. Statistical difference between pairs (paired Student's *t*-test) is shown as **P*<0.05, ***P*<0.01 and ****P*<0.005. (**D**) Visualization of GI-GFP localization relative to the presence of ZTL-LOV. GI-GFP was expressed with HA-ZTL-LOV or alone along with H2B-RFP in *N. benthamiana*, and GFP and RFP fluorescent signals were monitored by fluorescent microscopy. Signals from GFP, RFP, the merge, and the plot of GFP signals are shown. The surface plot of the GFP channel was generated using ImageJ software. Scale bars: 30 µm. These are representative of three independent experiments. (**E**) Nucleocytoplasmic distribution of GI-GFP protein depends on ZTL-LOV levels. ZTL LOV was co-expressed transiently with GI-GFP in *N. benthamiana* at different relative ratios. Numbers indicate the relative volume ratio of *Agrobacteria* containing ZTL-LOV to GI-GFP used for infiltration (ZTL to GI-GFP; 0: 0 to 1; 1: 1/32 to 1; 2: 1/16 to 1; 4: 1/8 to 1). Sample preparation and immunodetection were performed as described in A,B.

The long period phenotype in the LOV and LOV-F lines results from reduced ZTL levels (Fig. 2). However, the late flowering and long hypocotyls in these lines are not related to ZTL, because *ztl* null mutants have short hypocotyls and normal flowering in long days (Somers et al., 2004). Instead, these phenotypes are similar to plants lacking GI (Fowler et al., 1999; Huq et al., 2000; Martin-Tryon et al., 2007; Park et al., 1999). Because GI protein increases in *LOV-OX*, a change in availability and/or subcellular partitioning of GI might be responsible for the flowering time and hypocotyl phenotypes.

To address this, we tested the nucleocytoplasmic distribution of GI-HA in a stably transformed *LOV-OX* background. Relative to *GI:GI-HA* alone, cytosolic GI was increased, whereas nuclear GI was diminished (Fig. 5A, compare lanes 1 and 4 with 2 and 5). This confirmed the results of the transient assays (Fig. 4). The lower level of nuclear GI probably reduces the level of GI-FKF1 nuclear complexes in this background, leading to later flowering. Additionally, some ZTL-LOV is present in the nucleus (Fig. 4A), which might interfere with nuclear FKF1-GI interactions, further delaying flowering.

Finally, we tested how GI cytosolic and nuclear distribution is affected in the absence of ZTL by measuring GI-GFP partitioning in a *35S:GI-GFP ztl-103* background. Consistent with enhanced cytosolic GI distribution in *LOV-OX* plants, we observed more nuclear accumulation and cytosolic depletion of GI-GFP protein in the *ztl* mutant, relative to WT (Fig. 5B, compare lanes 1 and 3 with 2 and 4). Taken together, our data show that ZTL facilitates the retention and stabilization of GI in the cytosol (Fig. 6).

DISCUSSION

ZTL-mediated stabilization and cytosolic retention of GI

In this study, we uncovered two unexpected new roles for the F-box protein ZTL. We first observed that constitutive ectopic expression of the LOV and LOV-F domains of ZTL causes lengthening of the circadian period, delayed flowering in long days and elongated hypocotyls in red and blue light. Although endogenous ZTL levels are reduced in these lines, this combination of developmental and circadian defects is not associated with *ztl* mutants. ZTL deficiency is marked by long period, short hypocotyls in red light and normal to slightly early flowering in long days (Somers et al., 2000). Surprisingly, ectopic LOV domain expression also markedly increased levels of GI. However, neither can these three phenotypes be explained by high GI expression. GI-OX has little effect on flowering in long days and tends to slightly shorten both period and hypocotyl length (Mizoguchi et al., 2005). Instead, we propose that

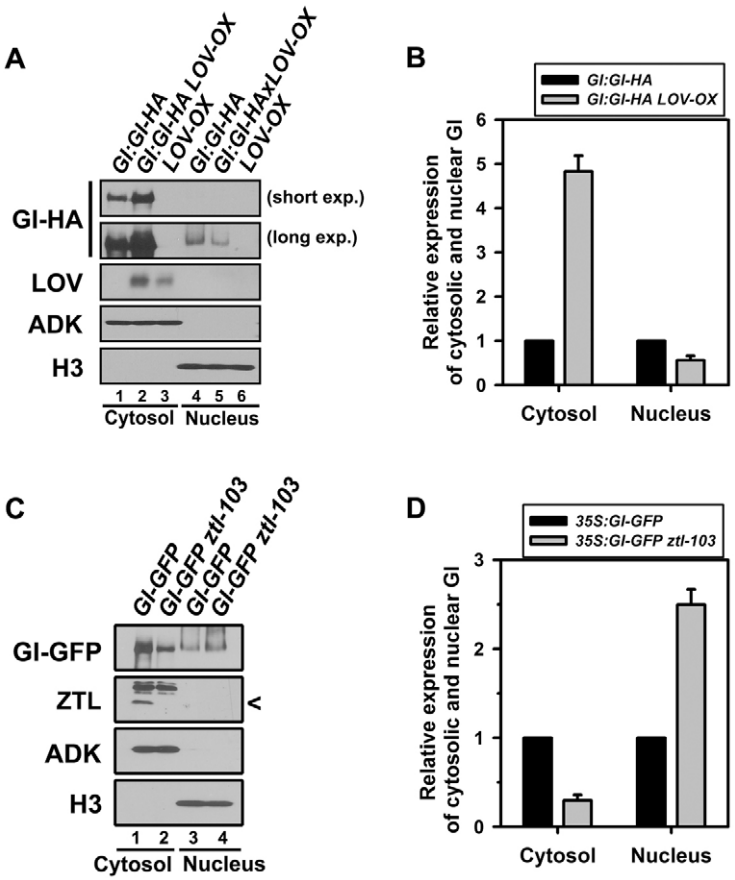

Fig. 5. ZTL skews nucleocytoplasmic distribution of GI to the cytosol in *Arabidopsis*. (**A**) Nucleocytoplasmic distribution of GI-HA protein in *GI:GI-HA*, *GI:GI-HAxLOV-OX* and *LOV-OX* plants. Each genotype was grown for 10 days in LD cycles and harvested at ZT13. GI-HA and LOV proteins were detected by immunoblotting. ADK and H3 were used as loading controls for cytosolic and nuclear proteins, respectively. Data are representative of three trials. (**B**) Relative expression of cytosolic and nuclear GI protein level from the blot shown in A. Levels of cytosolic and nuclear GI protein were normalized to ADK and H3, respectively and further normalized to GI-HA within a trial. Data are means ± s.e.m. of three independent trials. (**C**) Nucleocytoplasmic distribution of GI-GFP in *35S:GI-GFP* and *35S:GI-GFP/ztl-103* plants. Preparation of samples and immunodetection were performed as for A. Data are representative of three trials. In all immunoblots, ADK and H3 were used as normalization and loading controls for cytosolic and nuclear proteins, respectively. Arrowhead shows ZTL position. (**D**) Levels of cytosolic and nuclear GI normalized to ADK and H3, respectively, and further normalized to GI in *35S:GI-GFP* within a trial. Data are means ± s.e.m. of three independent trials.

these phenotypes result from the sequestration of GI into a LOV-GI complex. This prevents GI from carrying out its normal function and skews GI residence to the cytosol, depleting the nucleus of active GI. The developmental and circadian phenotypes of these lines phenocopy *gi* loss-of-function mutants, supporting this model (Fowler et al., 1999; Huq et al., 2000; Martin-Tryon et al., 2007; Park et al., 1999).

The first unexpected finding is the role of ZTL in the stabilization of GI. We have previously established that GI stabilizes ZTL protein and provided evidence that GI levels were diminished in a *ztl* background (Kim et al., 2007). Here, we confirm and extend this finding by showing that GI protein levels are significantly higher when a LOV-containing polypeptide is ectopically expressed at high levels in *Arabidopsis* plants, although *GI* mRNA transcript levels are unchanged (Fig. 3A,B). This supports the notion that LOV-domain interactions with GI are needed for GI accumulation. Additionally, transient expression of full-length ZTL and the ZTL LOV domain enhanced endogenous GI protein level by two to fourfold, whereas a non-GI interacting ZTL mutant (G46E) and the FKF1-LOV domain had little to no effect on GI accumulation (Fig. 3B-D). Taken together, these results show a specific and direct effect of ZTL on GI stabilization and indicate that ZTL is likely to be a limiting factor in controlling GI levels post-transcriptionally.

Second, we showed that transient expression of cytosol-localized ZTL or ZTL-LOV, but not nuclear-localized FKF1 nor non-interacting ZTL deletions and mutants, increases the cytosolic accumulation of GI while diminishing nuclear levels (Fig. 4A-D) and that these effects are ZTL-LOV dosage dependent (Fig. 4E). These transient assay results were supported by the observation that subcellular partitioning of GI in the LOV-OX background is shifted to the cytosol (Fig. 5A,B), and by the finding that GI nuclear levels are significantly higher than in the cytosol in *ztl-103* (Fig. 5C,D). These results indicate that a second novel and specific regulatory role of ZTL is the control of the nucleocytoplasmic partitioning of GI through LOV-mediated cytosolic retention (Fig. 6).

Interestingly, this dual effect of ZTL on GI is reminiscent of the relationship between FREQUENCY (FRQ) and an RNA helicase (FRH) in the *Neurospora* clock. The formation of a FRQ-FRH complex (FCC) helps stabilize and retain FRQ in the cytosol, with increased FRQ nuclear levels when the interaction is disrupted or FRH levels are low (Cha et al., 2011). Conversely, the mammalian clock component mCRY helps retain the nucleocytoplasmic protein mPER2 in the nucleus and away from ubiquitylation and degradation in the cytosol (Yagita et al., 2002). In both cases, one clock component simultaneously preferentially localizes and stabilizes a partner protein. These heterodimeric interactions between clock proteins appear to be a conserved feature among circadian systems, and might build a greater robustness into the network by increasing mutual dependencies and stabilities.

Regulation of flowering time and period by the ZTL family

Previous work has shown that ZTL, LKP2 and FKF1 have different primary roles in the control of flowering time and circadian period. *ztl* mutants have a significantly lengthened circadian period, with only slightly early flowering in short days, whereas *fkf1* mutants delay photoperiodic flowering time with marginal effects on circadian clock regulation (Baudry et al., 2010; Imaizumi et al., 2003; Kevei et al., 2006; Somers et al., 2000). *lkp2* mutants have little effect on either flowering time and circadian period, but

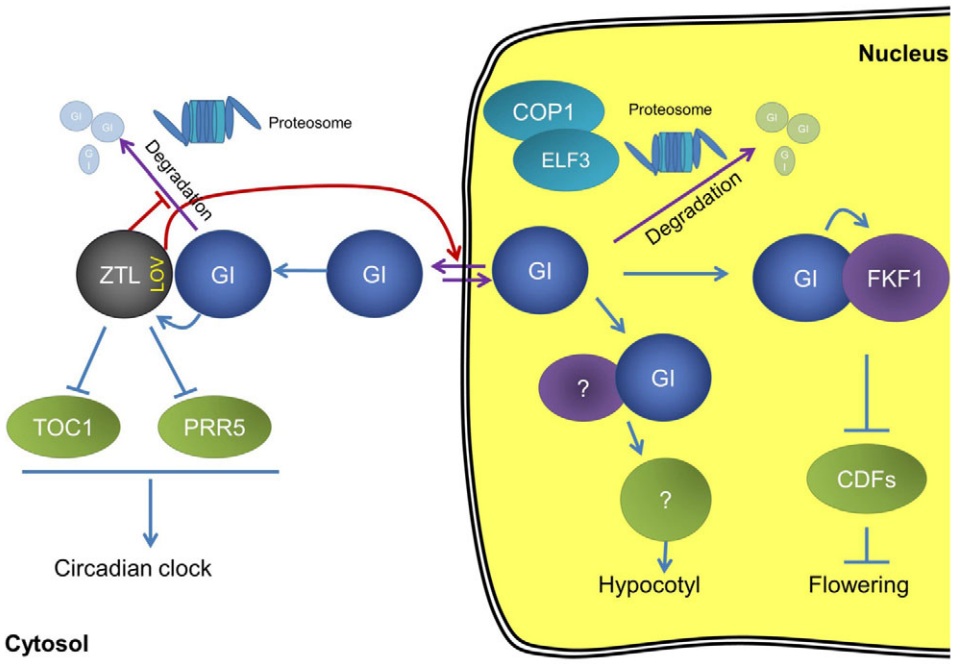

Fig. 6. Reciprocal regulation between GI and ZTL regulates the circadian clock and plant development. GI plays roles in the regulation of circadian period, photoperiod flowering and hypocotyl elongation, which depend on different partners in different cellular locations. Cytosolic GI and ZTL co-stabilize, leading to SCF^{ZTL} regulation of clock activity by facilitating TOC1 and PRR5 proteolysis. A nuclear GI-FKF1 complex promotes flowering by diminishing Cycling DOF Factor (CDF) levels. GI protein stabilizes ZTL and FKF1 protein in both compartments via LOV-domain mediated interactions in blue light. GI protein is destabilized by an ELF3-mediated SCF^{COP1} complex in the nucleus and by unknown interactions in the cytoplasm. The mechanism by which GI regulates hypocotyl elongation is unknown, but is indicated here as occurring in the nucleus for convenience. We propose additional layers of GI regulation through cytosolic retention of GI by ZTL and a concomitant inhibition of cytosolic GI degradation through a LOV domain-mediated interaction. Blue, purple and red arrows indicate functions of GI, regulations of GI abundance and partitioning, and ZTL-mediated GI regulation, respectively.

overexpression of LKP2 phenocopies ZTL overexpression (Imaizumi et al., 2003; Schultz et al., 2001; Takase et al., 2011).

Partial overlapping and redundant functions among these members in the regulation of the clock have been suggested by results showing *ztl fkf1* and *ztl fkf1 lkp2* genotypes have much longer periods and higher levels of TOC1 and PRR5 accumulation than do *ztl* mutants (Baudry et al., 2010). However, the functional relationships among these family members in flowering time control is less clear. Whereas *fkf1* mutants flower very late, *ztl lkp2* or *ztl* genotypes are early flowering in short days and these defects revert to very late flowering in the triple mutant (Fornara et al., 2009; Nelson et al., 2000; Takase et al., 2011).

Our findings now indicate that the early flowering phenotypes of the *ztl lkp2* and *ztl* genotypes are likely to be indirect effects of these mutations. In the absence of ZTL, GI partitioning shifts to the nucleus, even though total GI levels in the *ztl* mutant are lower (Fig. 5C) (Kim et al., 2007). These higher nuclear GI levels would enhance the formation of GI-FKF1 complexes and promote flowering. By contrast, both plants with ectopic LOV expression (Fig. 1) and ZTL-OX plants (Somers et al., 2004) are late flowering, consistent with increased GI sequestration to the cytosol, which would reduce nuclear GI-FKF1 complex formation. This would result in higher CDF accumulation and lower transcript levels of *CO* and *FT*.

ZTL OX also reduces the level of TOC1 and PRR5 (Kiba et al., 2007), which might explain the similarity to the late flowering phenotype of the *toc1 prr5* double mutant (Ito et al., 2008; Ito et al., 2012), For ZTL OX it is possible that both GI sequestration and reduced TOC1 and PRR5 act together to cause late flowering. However, ectopic expression of the ZTL-LOV domain, which also causes late flowering, cannot be attributed to reduction of TOC1 and PRR5 because it lacks the protein-interacting kelch domains.

The FKF1-dependent early flowering phenotypes of *ztl* or *ztl lkp2* can be explained by higher accumulation of GI, and a GI-FKF1 complex, in the nucleus of these mutants caused by loss of ZTL and LKP2 as sequestration factors. As well, increased cytosolic retention of FKF1 by direct interaction with cytosolic ZTL and/or LKP2 has been suggested (Takase et al., 2011) and would additionally contribute to controlling the nuclear levels of a GI-FKF1 complex by affecting FKF1, rather than GI, partitioning. These interpretations suggest that, unlike its role in period control, ZTL has no endogenous proteolytic targets directly related to flowering time control, but acts indirectly through complex formation and cytosolic retention of GI and, possibly, FKF1. These findings also act as a cautionary note when interpreting results from ectopic expression.

The GI-ZTL complex

ZTL is well established as a target-recruiting element of the E3 SCF complex, responsible for circadian-phase specific degradation of TOC1 and PRR5 (Somers et al., 2000; Han et al., 2004; Más et al., 2003; Kiba et al., 2007; Fujiwara et al., 2008). By contrast, GI is a biochemically unknown protein without well-characterized domains (Park et al., 1999; Fowler et al., 1999). *gi* mutations have no additional effect on period length in *ztl*

backgrounds and some *ZTL* mutations (e.g. G119D and G46E) reduce interaction with GI and compromise clock function (Kevei et al., 2006; Kim et al., 2007). These findings indicate that a direct interaction between GI and ZTL is necessary for clock control. However, it is not clear if GI and ZTL interact with targets together as a complex or whether they function separately as protein regulators. Overexpression of the LOV domain enhances cytosolic GI protein, but this stabilized GI is non-functional through sequestration by the LOV polypeptide from endogenous ZTL (Fig. 5A; Fig. 2D,E). This suggests that GI and ZTL might form, via the LOV domain, a strong and stable complex. We have previously shown that mild ZTL overexpression can still considerably shorten period by 2-4 hours (Somers et al., 2004). This might result from an effect of GI, through a GI-ZTL complex, on ZTL activity beyond simple stabilization and increase of ZTL levels.

Alternatively, a GI-ZTL complex might function as a reservoir of ZTL in the cytoplasm. Light conditions combined with clock-controlled expression of *GI* might indirectly regulate interactions between ZTL and its other protein partners. In darkness, the ZTL-GI interaction is weaker and the complex may dissociate more easily and favor ZTL substrate (TOC1, PRR5) or ZTL-ASK interactions predominantly, or newly dark-synthesized ZTL might preferentially complex with these factors over GI.

Whereas cytoplasmic ZTL affects stability and nucleocytoplasmic distribution of GI, nuclear-localized FKF1 has a minor effect on GI (Fig. 3D; Fig. 4C). This is consistent with little or no clock-related phenotypes in *fkf1* mutants or FKF1 overexpressors (Imaizumi et al., 2003). In addition, FKF1 overexpressors have nearly normal flowering time, whereas overexpression of both FKF1 and GI induces dramatically early flowering (Sawa et al., 2007), indicating that FKF1 alone is unlikely to affect GI levels or activity strongly. As with ZTL, GI stabilizes FKF1 (Fornara et al., 2009), but the levels of GI in the *fkf1* mutant or FKF1 overexpressor have not been tested.

The ZTL family of F-box proteins as stabilizing factors

Although ZTL targets TOC1 and PRR5 for degradation, our results show that ZTL can also stabilize proteins (GI). In addition to interacting with the ZTL protein family, GI-ELF4 complexes regulate GI subnuclear positioning and GI is de-stabilized by an ELF3-COP1 complex in the nucleus (Kim et al., 2013; Yu et al., 2008). Considering that ELF3 and COP1 exist predominantly in the nucleus, ZTL might enhance overall GI protein levels by facilitating cytosolic retention of GI protein and sequestering it from proteolysis by SCF^{COP1}. ZTL might additionally stabilize GI by further sequestration from degradation by an unknown cytosolic mechanism (Fig. 6).

A stabilizing effect on CO by FKF1 has been reported recently (Song et al., 2012). A blue light-dependent FKF1-CO interaction drives accumulation of CO protein in the late afternoon, which mediates control of day length-dependent flowering time. At the same time, FKF1 destabilizes CDFs through kelch-mediated interactions, mostly at the end of day (Imaizumi et al., 2005). It appears, then, that the ZTL family of F-box proteins can have contrasting effects on interaction partners, either to recruit them towards or sequester them from proteolysis.

Acknowledgements
We thank Dr Hong Gil Nam for the kind donation of the Gateway version of pCsVMV:GFP-C-999 and pCsVMV:HA-C-1300 and Dr Chentao Lin for *cry1-304*.

Funding
This work was supported by grants from the National Science Foundation [IOB-0344377 to D.E.S.]; the National Institutes of Health [R01GM093285 to D.E.S.]; and the World Class University Program of South Korea [No. R31-2008–000–10105–0 to D.E.S.]. Deposited in PMC for release after 12 months.

Competing interests statement
The authors declare no competing financial interests.

Author contributions
J.K., R.G. and D.E.S. contributed to project design. J.K, R.G. and R.A.G. carried out experiments. J.K., R.G. and D.E.S. wrote the manuscript. All authors discussed the results.

Supplementary material
Supplementary material available online at
http://dev.biologists.org/lookup/suppl/doi:10.1242/dev.096651/-/DC1

References

Ballario, P., Vittorioso, P., Magrelli, A., Talora, C., Cabibbo, A. and Macino, G. (1996). White collar-1, a central regulator of blue light responses in Neurospora, is a zinc finger protein. *EMBO J.* **15**, 1650-1657.
Ballario, P., Talora, C., Galli, D., Linden, H. and Macino, G. (1998). Roles in dimerization and blue light photoresponse of the PAS and LOV domains of Neurospora crassa white collar proteins. *Mol. Microbiol.* **29**, 719-729.
Baudry, A., Ito, S., Song, Y. H., Strait, A. A., Kiba, T., Lu, S., Henriques, R., Pruneda-Paz, J. L., Chua, N. H., Tobin, E. M. et al. (2010). F-box proteins FKF1 and LKP2 act in concert with ZEITLUPE to control Arabidopsis clock progression. *Plant Cell* **22**, 606-622.
Cha, J., Yuan, H. and Liu, Y. (2011). Regulation of the activity and cellular localization of the circadian clock protein FRQ. *J. Biol. Chem.* **286**, 11469-11478.
Clough, S. J. and Bent, A. F. (1998). Floral dip: a simplified method for Agrobacterium-mediated transformation of Arabidopsis thaliana. *Plant J.* **16**, 735-743.
Crosson, S., Rajagopal, S. and Moffat, K. (2003). The LOV domain family: photoresponsive signaling modules coupled to diverse output domains. *Biochemistry* **42**, 2-10.
David, K. M., Armbruster, U., Tama, N. and Putterill, J. (2006). Arabidopsis GIGANTEA protein is post-transcriptionally regulated by light and dark. *FEBS Lett.* **580**, 1193-1197.
Demarsy, E. and Fankhauser, C. (2009). Higher plants use LOV to perceive blue light. *Curr. Opin. Plant Biol.* **12**, 69-74.
Fornara, F., Panigrahi, K. C., Gissot, L., Sauerbrunn, N., Rühl, M., Jarillo, J. A. and Coupland, G. (2009). Arabidopsis DOF transcription factors act redundantly to reduce CONSTANS expression and are essential for a photoperiodic flowering response. *Dev. Cell* **17**, 75-86.
Fowler, S., Lee, K., Onouchi, H., Samach, A., Richardson, K., Morris, B., Coupland, G. and Putterill, J. (1999). GIGANTEA: a circadian clock-controlled gene that regulates photoperiodic flowering in Arabidopsis and encodes a protein with several possible membrane-spanning domains. *EMBO J.* **18**, 4679-4688.
Fujiwara, S., Wang, L., Han, L., Suh, S. S., Salomé, P. A., McClung, C. R. and Somers, D. E. (2008). Post-translational regulation of the Arabidopsis circadian clock through selective proteolysis and phosphorylation of pseudo-response regulator proteins. *J. Biol. Chem.* **283**, 23073-23083.
Godinho, S. I., Maywood, E. S., Shaw, L., Tucci, V., Barnard, A. R., Busino, L., Pagano, M., Kendall, R., Quwailid, M. M., Romero, M. R. et al. (2007). The after-hours mutant reveals a role for Fbxl3 in determining mammalian circadian period. *Science* **316**, 897-900.
Han, L., Mason, M., Risseeuw, E. P., Crosby, W. L. and Somers, D. E. (2004). Formation of an SCF(ZTL) complex is required for proper regulation of circadian timing. *Plant J.* **40**, 291-301.
Harmer, S. L. (2009). The circadian system in higher plants. *Annu. Rev. Plant Biol.* **60**, 357-377.
He, Q., Cheng, P., Yang, Y., Wang, L., Gardner, K. H. and Liu, Y. (2002). White collar-1, a DNA binding transcription factor and a light sensor. *Science* **297**, 840-843.
He, Q., Cheng, P., Yang, Y., He, Q., Yu, H. and Liu, Y. (2003). FWD1-mediated degradation of FREQUENCY in Neurospora establishes a conserved mechanism for circadian clock regulation. *EMBO J.* **22**, 4421-4430.
Herrero, E. and Davis, S. J. (2012). Time for a nuclear meeting: protein trafficking and chromatin dynamics intersect in the plant circadian system. *Mol. Plant* **5**, 554-565.
Huq, E., Tepperman, J. M. and Quail, P. H. (2000). GIGANTEA is a nuclear protein involved in phytochrome signaling in Arabidopsis. *Proc. Natl. Acad. Sci. USA* **97**, 9789-9794.
Imaizumi, T., Tran, H. G., Swartz, T. E., Briggs, W. R. and Kay, S. A. (2003). FKF1 is essential for photoperiodic-specific light signalling in Arabidopsis. *Nature* **426**, 302-306.

Imaizumi, T., Schultz, T. F., Harmon, F. G., Ho, L. A. and Kay, S. A. (2005). FKF1 F-box protein mediates cyclic degradation of a repressor of CONSTANS in Arabidopsis. *Science* **309**, 293-297.
Ito, S., Niwa, Y., Nakamichi, N., Kawamura, H., Yamashino, T. and Mizuno, T. (2008). Insight into missing genetic links between two evening-expressed pseudo-response regulator genes TOC1 and PRR5 in the circadian clock-controlled circuitry in Arabidopsis thaliana. *Plant Cell Physiol.* **49**, 201-213.
Ito, S., Song, Y. H. and Imaizumi, T. (2012). LOV domain-containing F-box proteins: light-dependent protein degradation modules in Arabidopsis. *Mol. Plant* **5**, 573-582.
Kevei, E., Gyula, P., Hall, A., Kozma-Bognár, L., Kim, W. Y., Eriksson, M. E., Tóth, R., Hanano, S., Fehér, B., Southern, M. M. et al. (2006). Forward genetic analysis of the circadian clock separates the multiple functions of ZEITLUPE. *Plant Physiol.* **140**, 933-945.
Kiba, T., Henriques, R., Sakakibara, H. and Chua, N. H. (2007). Targeted degradation of PSEUDO-RESPONSE REGULATOR5 by an SCFZTL complex regulates clock function and photomorphogenesis in Arabidopsis thaliana. *Plant Cell* **19**, 2516-2530.
Kim, J. and Somers, D. E. (2010). Rapid assessment of gene function in the circadian clock using artificial microRNA in Arabidopsis mesophyll protoplasts. *Plant Physiol.* **154**, 611-621.
Kim, W. Y., Fujiwara, S., Suh, S. S., Kim, J., Kim, Y., Han, L., David, K., Putterill, J., Nam, H. G. and Somers, D. E. (2007). ZEITLUPE is a circadian photoreceptor stabilized by GIGANTEA in blue light. *Nature* **449**, 356-360.
Kim, J., Kim, Y., Yeom, M., Kim, J. H. and Nam, H. G. (2008). FIONA1 is essential for regulating period length in the Arabidopsis circadian clock. *Plant Cell* **20**, 307-319.
Kim, Y., Lim, J., Yeom, M., Kim, H., Kim, J., Wang, L., Kim, W. Y., Somers, D. E. and Nam, H. G. (2013). ELF4 regulates GIGANTEA chromatin access through subnuclear sequestration. *Cell Rep.* **3**, 671-677.
Ko, H. W., Jiang, J. and Edery, I. (2002). Role for Slimb in the degradation of Drosophila Period protein phosphorylated by Doubletime. *Nature* **420**, 673-678.
Koh, K., Zheng, X. and Sehgal, A. (2006). JETLAG resets the Drosophila circadian clock by promoting light-induced degradation of TIMELESS. *Science* **312**, 1809-1812.
Martin-Tryon, E. L., Kreps, J. A. and Harmer, S. L. (2007). GIGANTEA acts in blue light signaling and has biochemically separable roles in circadian clock and flowering time regulation. *Plant Physiol.* **143**, 473-486.
Más, P. (2008). Circadian clock function in Arabidopsis thaliana: time beyond transcription. *Trends Cell Biol.* **18**, 273-281.
Más, P., Kim, W. Y., Somers, D. E. and Kay, S. A. (2003). Targeted degradation of TOC1 by ZTL modulates circadian function in Arabidopsis thaliana. *Nature* **426**, 567-570.
Matsuoka, D. and Tokutomi, S. (2005). Blue light-regulated molecular switch of Ser/Thr kinase in phototropin. *Proc. Natl. Acad. Sci. USA* **102**, 13337-13342.
Mizoguchi, T., Wright, L., Fujiwara, S., Cremer, F., Lee, K., Onouchi, H., Mouradov, A., Fowler, S., Kamada, H., Putterill, J. et al. (2005). Distinct roles of GIGANTEA in promoting flowering and regulating circadian rhythms in Arabidopsis. *Plant Cell* **17**, 2255-2270.
Mouradov, A., Cremer, F. and Coupland, G. (2002). Control of flowering time: interacting pathways as a basis for diversity. *Plant Cell* **14** Suppl., S111-S130.
Nakasako, M., Zikihara, K., Matsuoka, D., Katsura, H. and Tokutomi, S. (2008). Structural basis of the LOV1 dimerization of Arabidopsis phototropins 1 and 2. *J. Mol. Biol.* **381**, 718-733.
Neff, M. M. and Chory, J. (1998). Genetic interactions between phytochrome A, phytochrome B, and cryptochrome 1 during Arabidopsis development. *Plant Physiol.* **118**, 27-35.
Nelson, D. C., Lasswell, J., Rogg, L. E., Cohen, M. A. and Bartel, B. (2000). FKF1, a clock-controlled gene that regulates the transition to flowering in Arabidopsis. *Cell* **101**, 331-340.
Park, D. H., Somers, D. E., Kim, Y. S., Choy, Y. H., Lim, H. K., Soh, M. S., Kim, H. J., Kay, S. A. and Nam, H. G. (1999). Control of circadian rhythms and photoperiodic flowering by the Arabidopsis GIGANTEA gene. *Science* **285**, 1579-1582.
Sawa, M., Nusinow, D. A., Kay, S. A. and Imaizumi, T. (2007). FKF1 and GIGANTEA complex formation is required for day-length measurement in Arabidopsis. *Science* **318**, 261-265.
Schultz, T. F., Kiyosue, T., Yanovsky, M., Wada, M. and Kay, S. A. (2001). A role for LKP2 in the circadian clock of Arabidopsis. *Plant Cell* **13**, 2659-2670.
Siepka, S. M., Yoo, S. H., Park, J., Song, W., Kumar, V., Hu, Y., Lee, C. and Takahashi, J. S. (2007). Circadian mutant Overtime reveals F-box protein FBXL3 regulation of cryptochrome and period gene expression. *Cell* **129**, 1011-1023.
Somers, D. E., Schultz, T. F., Milnamow, M. and Kay, S. A. (2000). *ZEITLUPE* encodes a novel clock-associated PAS protein from *Arabidopsis*. *Cell* **101**, 319-329.
Somers, D. E., Kim, W. Y. and Geng, R. (2004). The F-box protein ZEITLUPE confers dosage-dependent control on the circadian clock, photomorphogenesis, and flowering time. *Plant Cell* **16**, 769-782.
Song, Y. H., Smith, R. W., To, B. J., Millar, A. J. and Imaizumi, T. (2012). FKF1 conveys timing information for CONSTANS stabilization in photoperiodic flowering. *Science* **336**, 1045-1049.
Takase, T., Nishiyama, Y., Tanihigashi, H., Ogura, Y., Miyazaki, Y., Yamada, Y. and Kiyosue, T. (2011). LOV KELCH PROTEIN2 and ZEITLUPE repress Arabidopsis photoperiodic flowering under non-inductive conditions, dependent on FLAVIN-BINDING KELCH REPEAT F-BOX1. *Plant J.* **67**, 608-621.
Tataroğlu, O. and Schafmeier, T. (2010). Of switches and hourglasses: regulation of subcellular traffic in circadian clocks by phosphorylation. *EMBO Rep.* **11**, 927-935.
Voinnet, O., Rivas, S., Mestre, P. and Baulcombe, D. (2003). An enhanced transient expression system in plants based on suppression of gene silencing by the p19 protein of tomato bushy stunt virus. *Plant J.* **33**, 949-956.
Wang, L., Fujiwara, S. and Somers, D. E. (2010). PRR5 regulates phosphorylation, nuclear import and subnuclear localization of TOC1 in the Arabidopsis circadian clock. *EMBO J.* **29**, 1903-1915.
Yagita, K., Tamanini, F., Yasuda, M., Hoeijmakers, J. H., van der Horst, G. T. and Okamura, H. (2002). Nucleocytoplasmic shuttling and mCRY-dependent inhibition of ubiquitylation of the mPER2 clock protein. *EMBO J.* **21**, 1301-1314.
Yakir, E., Hilman, D., Harir, Y. and Green, R. M. (2007). Regulation of output from the plant circadian clock. *FEBS J.* **274**, 335-345.
Yu, J. W., Rubio, V., Lee, N. Y., Bai, S., Lee, S. Y., Kim, S. S., Liu, L., Zhang, Y., Irigoyen, M. L., Sullivan, J. A. et al. (2008). COP1 and ELF3 control circadian function and photoperiodic flowering by regulating GI stability. *Mol. Cell* **32**, 617-630.

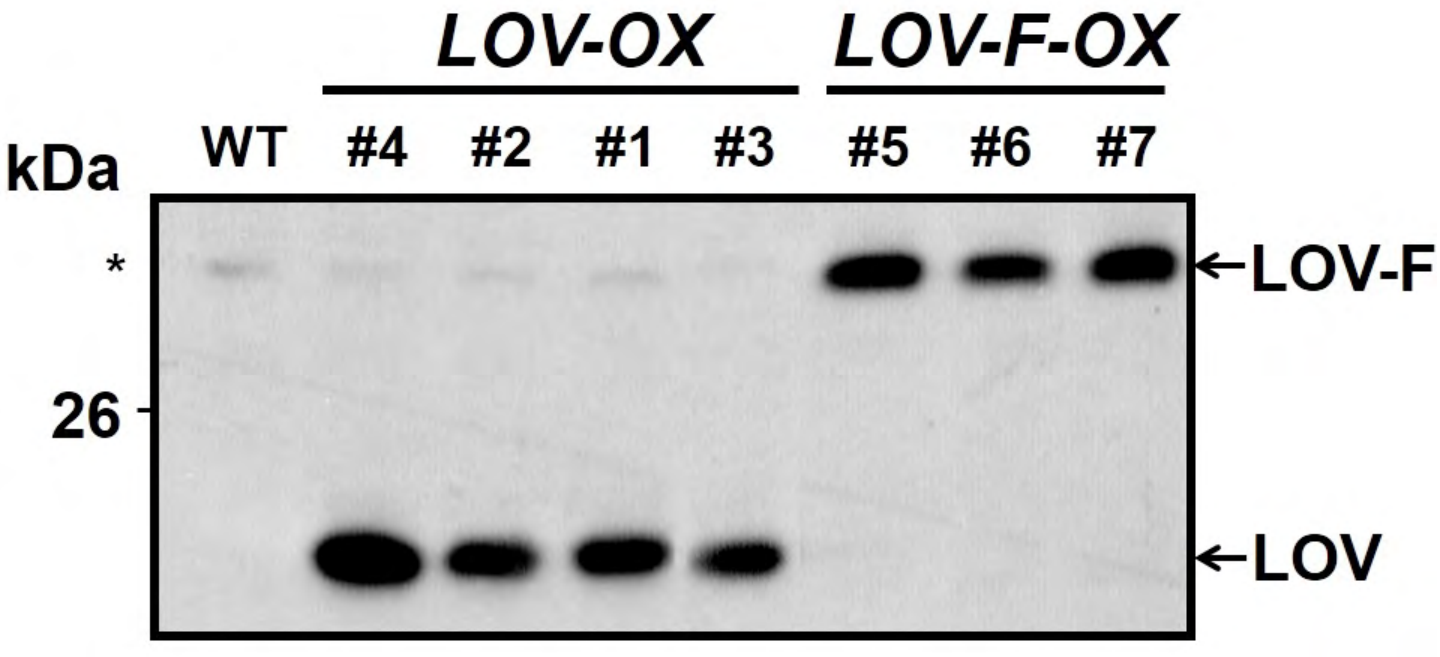

Fig. S1. Identification of independent transgenic lines expressing LOV and LOV-F domains of ZTL. The accumulation of LOV and LOV-F polypeptides was detected using anti-ZTL antibody from total protein extracts of four LOV-expressing lines (#4, #2, #1, and #3) and three LOV-F expressing lines (#5, #6, and #7). A weak band (*) was occasionally detected in WT extracts at the same running position as that of LOV-F polypeptide.

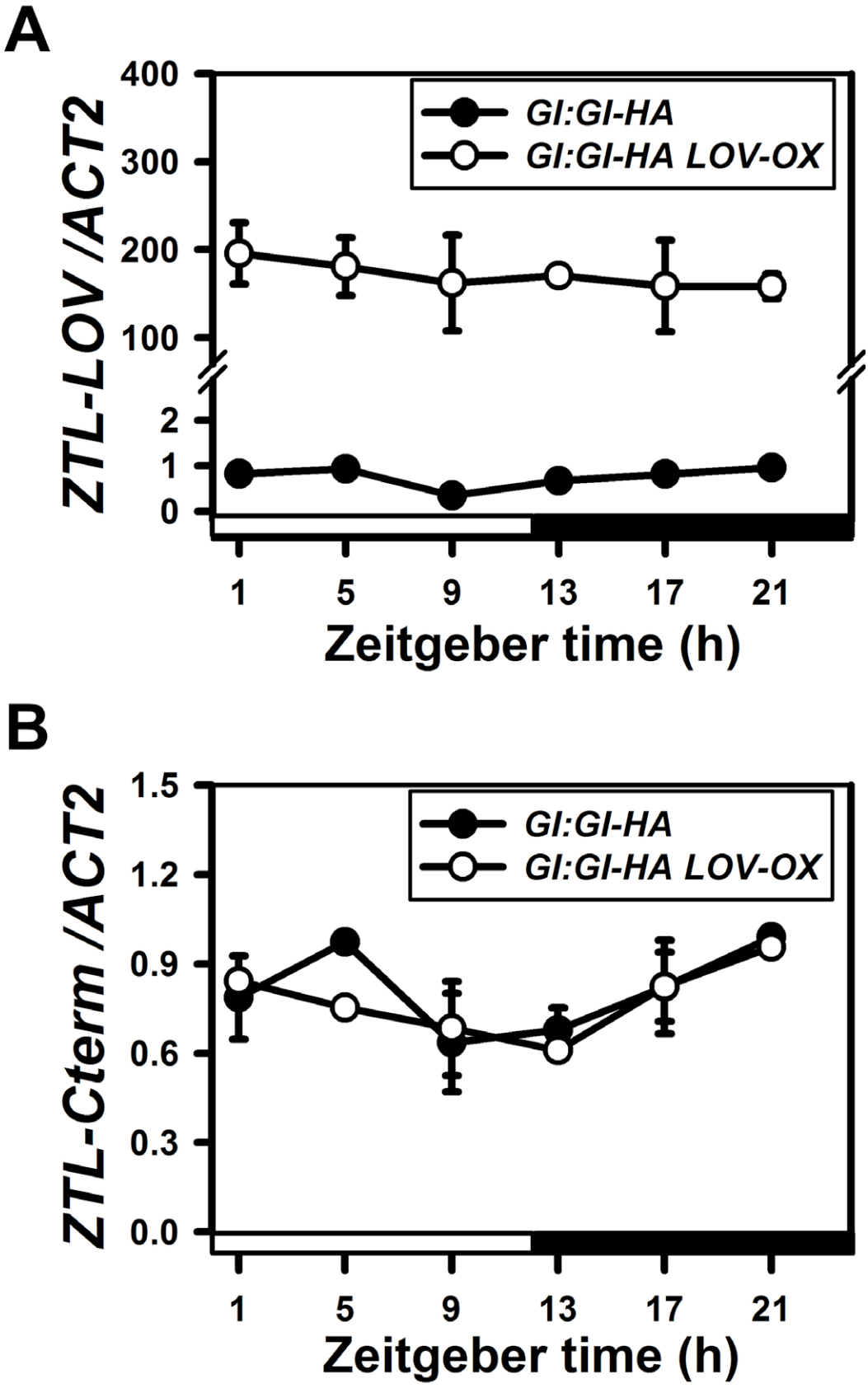

Fig. S2. Accumulation of endogenous *ZTL* mRNA is unchanged in *GI:GI-HA x LOV-OX*. Expression of LOV (**A**) and endogenous *ZTL* (**B**) mRNA levels in *GI:GI-HA x LOV-OX* and *GI:GI-HA* plants. Expression of introduced LOV and endogenous ZTL transcripts was monitored from the same cDNAs used in Fig 3B using primer sets detecting the LOV and KELCH domains of ZTL, respectively. Relative expression was calculated by normalization to ACT2 and then normalized to highest level among WT samples within a trial. Data indicate means±SEM of two independent trials.

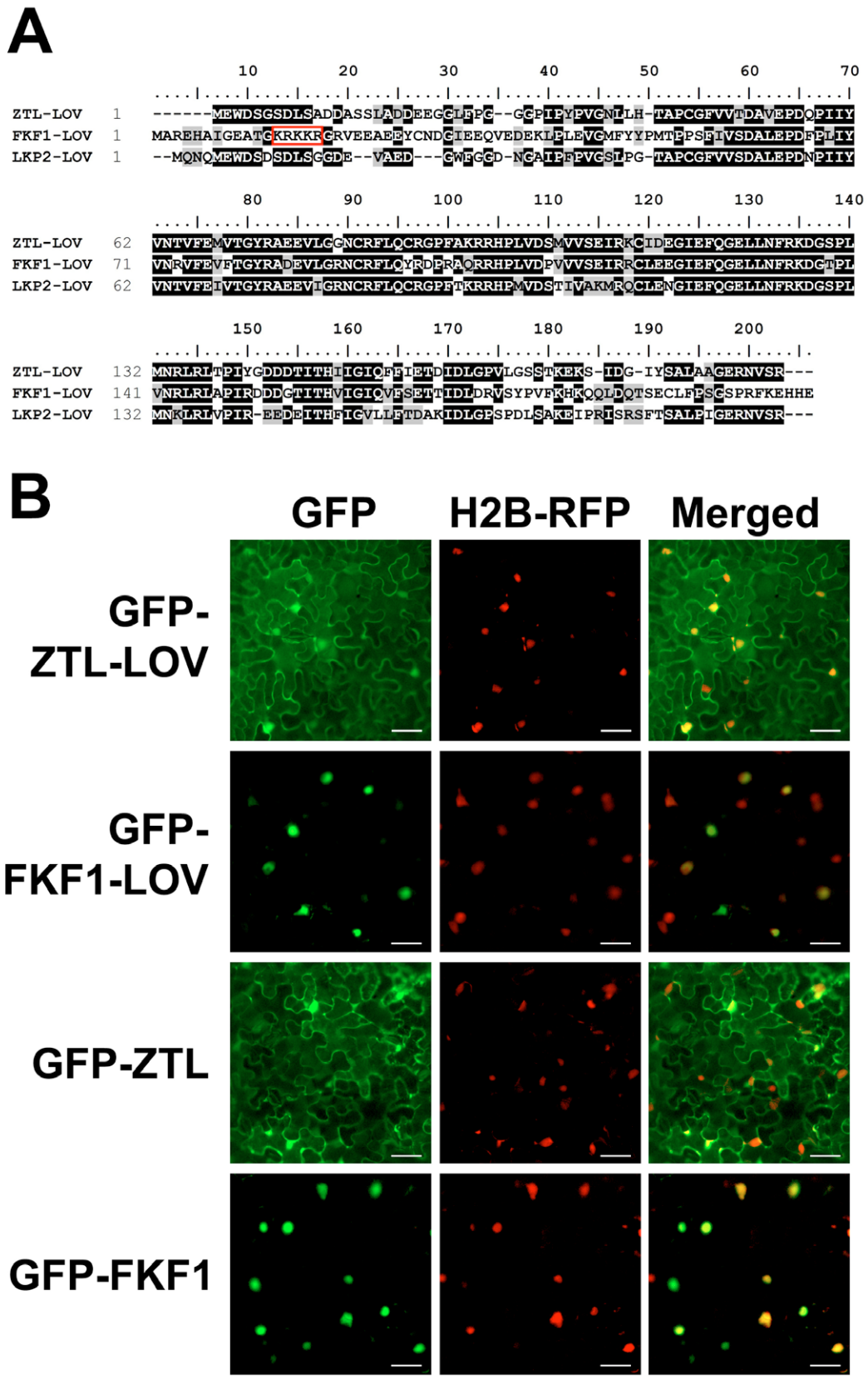

Fig. S3. Subcellular localization of full length or the LOV domain of ZTL and FKF1. (**A**) Sequence alignment of ZTL and FKF1 LOV domains. Putative NLS is marked with a box. (**B**) Localization of full length or LOV domain of ZTL and FKF1. GFP-ZTL-LOV, GFP-FKF1-LOV, GFP-ZTL or GFP-FKF1 were co-expressed with H2B-RFP transiently in *N. benthamina* and GFP and RFP fluorescent signals were monitored with a fluorescent microscope. Signals from GFP, RFP, and the merged signals are shown. Scale bars = 30 um. These are representative of three independent experiments.

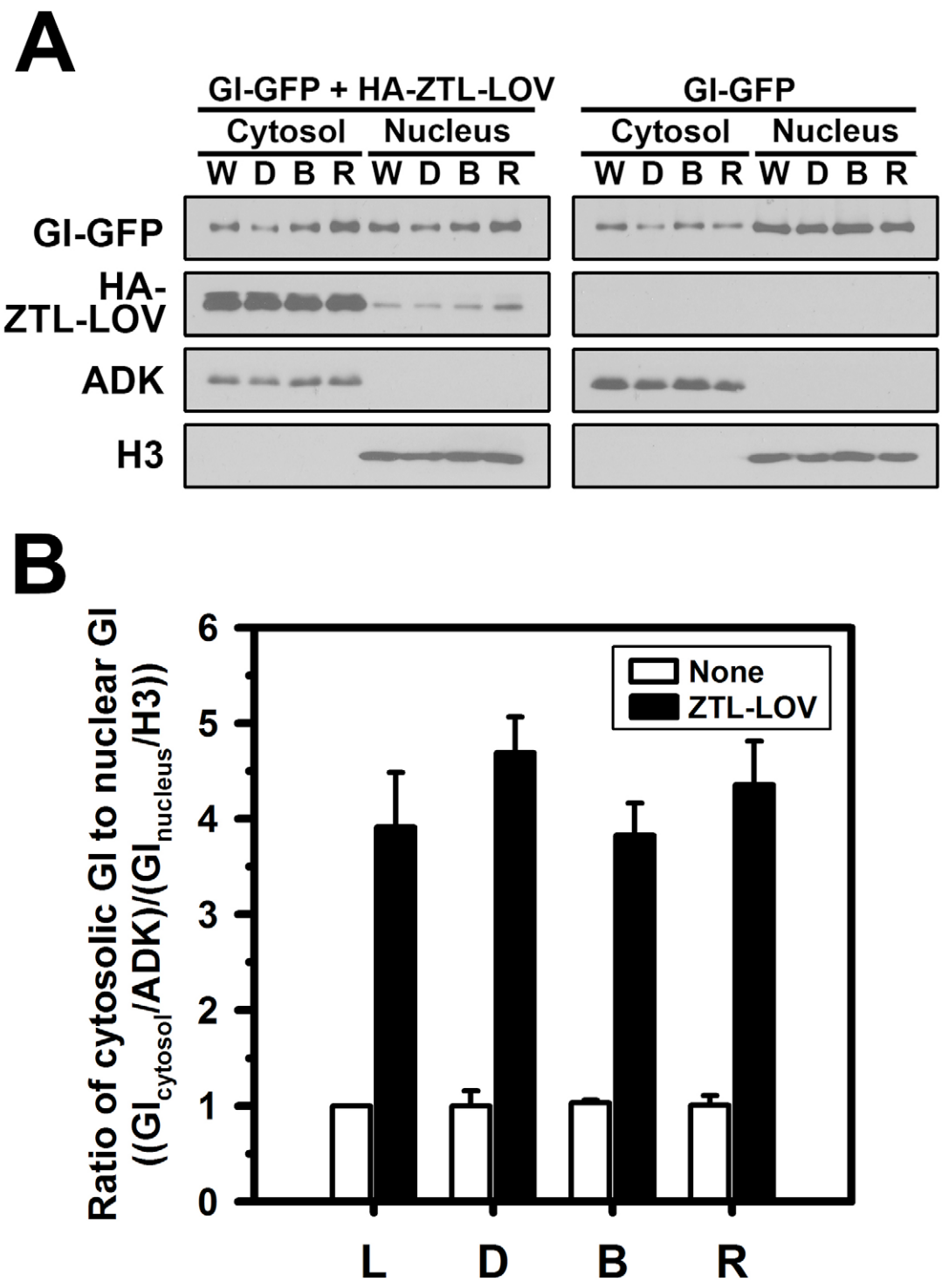

Fig. S4. Light quality has no effect on ZTL-LOV-dependent GI localization. (**A**) Cytosolic and nuclear GI-GFP protein levels in *N. benthamiana* transiently expressing GI-GFP along HA-ZTL-LOV as effectors in the different light conditions. *35S:GI-GFP* was expressed alone or co-expressed with *CsVMV:HA-ZTL-LOV* plasmids in *N. benthamiana*. After 48 h incubation, plants were shifted to chambers with irradiations as indicated (L: White light; D: Dark; B: Blue; R Red) for 6 hours from ZT0. Data are representative of two trials. (**B**) Quantification of ratios of cytosolic to nuclear GI level from (A). Levels of cytosolic and nuclear GI protein normalized to ADK and H3, respectively and further normalized to a non-effector sample (None) within a trial. Bars show means ± SEM of two independent trials.

Table S1. Primers used in this study

1. Plasmid construction

Primer name	Sequences (5′ to 3′)*	R.E.	Vector
ZTL-F	TCCGGATCCTTATGGAGTGGGACAGTGGT	*Bam*HI	pCR-CCD-F
ZTL-R	TCCAGGCCTTTACGTGAGATAGCTCGCTA	*Stu*I	
FKF1-F	TCCACTAGTGTCGACATGGCGAGAGAACATGC	*Spe*I	pCR-CCD-F
FKF1-R	TCCAGGCCTTTACAGATCCGAGTCTTG	*Stu*I	
FKF1-LOV-F	CTTCTGCAGATGGCGAGAGAACATGCGATC	*Pst*I	pCR-CCD-F
FKF1-LOV-R	CTTAGGCCTTCATTCATGATGCTCCTTAAACCT	*Stu*I	
ZTL-LOV-F	CTTCTGCAGATGGAGTGGGACAGTGGTTCC	*Pst*I	pCR-CCD-F
ZTL-LOV-R	CTTAGGCCTTCATCGGGAAACATTCCGCTCCC	*Stu*I	
ZTL-Kelch-F	CTTGGATCCATGACCACCCTTGAAGCT	*Bam*HI	pCR-CCD-F
ZTL-Kelch-R	CTTAGGCCTTTACGTGAGATAGCTCGCTA	*Stu*I	

*Annealing temperature for all primers is 56℃
R.E., restriction enzyme sites

2. RT-PCR or real-time PCR

Primer name	Sequences (5′ to 3′)	Annealing temperature
CO-RT-F	ACGCCATCAGCGAGTTCC	48℃
CO-RT-R	AAATGTATGCGTTATGGTTAATGG	
FT-RT-F	ACAACTGGAACAACCTTTGGCAATG	60℃
FT-RT-R	ACTACTATAGGCATCATCACCGTTCGTTACTCG	
ACT2-RT-F	AAAACCACTTACAGAGTTCGTTCG	55℃
ACT2-RT-R	GTTGAACGGAAGGGATTGAGAGT	
HA-qPCR-F	GGACTACGCTTCTTTGGGTGG	60℃
HA-qPCR-R	GGATAGCCCGCATAGTCAGGAAC	
ZTL-LOV-qPCR-F	TCCGGATCCTTATGGAGTGGGACAGTGGT	60℃
ZTL-LOV-qPCR-R	CCTCCGAGAACTTCCTCAG	
ZTL-KELCH-qPCR-F	TCTTGATATTTGGCGGCTCAGT	60℃
ZTL-KELCH-qPCR-R	TTGTCCTCCGTTGGGTCAAGTA	
ACT2-qPCR-F	CAGTGTCTGGATCGGAGGAT	60℃
ACT2-qPCR-R	TGAACAATCGATGGACCTGA	